Am J Physiol Regul Integr Comp Physiol 293: R2090–R2098, 2007.
First published August 29, 2007; doi:10.1152/ajpregu.00166.2007.

Canine erythrocytes express the $P2X_7$ receptor: greatly increased function compared with human erythrocytes

Ronald Sluyter,[1] Anne N. Shemon,[1] William E. Hughes,[2,3] Ryan O. Stevenson,[1,4] Jennifer G. Georgiou,[1] Guy D. Eslick,[1] Rosanne M. Taylor,[4] and James S. Wiley[1]

[1]*Department of Medicine, Nepean Clinical School, University of Sydney, Penrith;* [2]*Phospholipid Biology Group, The Garvan Institute of Medical Research, Sydney;* [3]*Department of Medicine, University of New South Wales, St Vincent's Hospital, Sydney; and* [4]*Faculty of Veterinary Science, University of Sydney, New South Wales, Australia*

Submitted 6 March 2007; accepted in final form 20 August 2007

Sluyter R, Shemon AN, Hughes WE, Stevenson RO, Georgiou JG, Eslick GD, Taylor RM, Wiley JS. Canine erythrocytes express the $P2X_7$ receptor: greatly increased function compared with human erythrocytes. *Am J Physiol Regul Integr Comp Physiol* 293: R2090–R2098, 2007. First published August 29, 2007; doi:10.1152/ajpregu.00166.2007.—Over three decades ago, Parker and Snow (*Am J Physiol* 223: 888–893, 1972) demonstrated that canine erythrocytes undergo an increase in cation permeability when incubated with extracellular ATP. In this study we examined the expression and function of the channel/pore-forming $P2X_7$ receptor on canine erythrocytes. $P2X_7$ receptors were detected on canine erythrocytes by immunocytochemistry and immunoblotting. Extracellular ATP induced $^{86}Rb^+$ (K^+) efflux from canine erythrocytes that was 20 times greater than that from human erythrocytes. The $P2X_7$ agonist 2′(3′)-*O*-(4-benzoylbenzoyl)adenosine 5′-trisphosphate (BzATP) was more potent than ATP, and both stimulated $^{86}Rb^+$ efflux from erythrocytes in a dose-dependent fashion with EC_{50} values of ~7 and ~309 μM, respectively. 2-Methylthioadenosine 5′-triphosphate and adenosine 5′-*O*-(3-thiotriphosphate) induced a smaller $^{86}Rb^+$ efflux from erythrocytes, whereas ADP, AMP, UTP, or adenosine had no effect. ATP-induced $^{86}Rb^+$ efflux from erythrocytes was inhibited by oxidized ATP, KN-62, and Brilliant blue G, known $P2X_7$ antagonists. ATP also induced uptake of choline$^+$ into canine erythrocytes that was 60 times greater than that into human erythrocytes. Overnight incubation of canine erythrocytes with ATP and BzATP induced phosphatidylserine exposure in >80% of cells and caused up to 20% hemolysis. In contrast, <30% of human erythrocytes showed phosphatidylserine exposure after overnight incubation with ATP and BzATP, and hemolysis was negligible. Flow cytometric measurements of ATP-induced ethidium$^+$ uptake showed that $P2X_7$ function was three times lower in canine monocytes than in human monocytes. These data show that the massive cation permeability increase induced by extracellular ATP in canine erythrocytes results from activation and opening of the $P2X_7$ receptor channel/pore.

purinergic receptor; P2Z receptor; extracellular adenosine 5′-triphosphate; red blood cell; dog

THE P2X RECEPTOR FAMILY ($P2X_1$ to $P2X_7$) of ligand-gated cation channels are emerging as important molecules in health and disease (31). The $P2X_7$ receptor has been cloned and expressed from rat (57), human (46), mouse (7), *Xenopus* (44), zebrafish (33), and seabream (39). Like other P2X receptor members, the $P2X_7$ receptor has intracellular amino and carboxyl termini with two hydrophobic membrane-spanning domains, separated by a long, glycosylated extracellular loop containing the proposed ATP-binding sites (42). The $P2X_7$ receptor differs from other P2X receptors, having a relatively low affinity for ATP and a rank order of agonist potency of 2′(3′)-*O*-(4-benzoylbenzoyl)adenosine 5′-trisphosphate (BzATP) > ATP > 2-methylthioadenosine 5′-trisphosphate (2MeSATP) > adenosine 5′-*O*-(3-thiotriphosphate) (ATPγS) (7, 46, 57). Activation of $P2X_7$ opens a cation-selective channel, allowing an influx of Ca^{2+} and Na^+ and efflux of K^+ (7, 46, 57). Prolonged exposure to ATP induces a second permeability state, which allows the uptake of larger cations such as choline$^+$, ethidium$^+$, and Yo-Pro-1^{2+} (7, 10, 15, 46, 57). Whether this second permeability state is due to dilatation of the $P2X_7$ channel or activation/recruitment of a second molecule is the subject of much debate (29, 42, 55), although recent data indicate that pannexin-1 is the pore-forming unit of the $P2X_7$ receptor (45). A range of downstream events follow $P2X_7$ activation, including phosphatidylserine (PS) exposure and cell lysis (8).

The $P2X_7$ receptor is predominately expressed on mononuclear leukocytes but can be present on other cell types (5). Our laboratory has shown that human erythrocytes express relatively low levels of $P2X_7$ receptors compared with mononuclear leukocytes (52) and that activation of this receptor mediates cation fluxes (52) and PS exposure in these cells (54). Some 35 years ago, Parker and Snow reported in this journal that canine erythrocytes undergo an increase in cation permeability when incubated with extracellular ATP but not other nucleotides (43). The gene coding the $P2X_7$ receptor has been identified in the canine genome (36), and $P2X_7$ transcripts have been detected in canine brain (35), indicating that the $P2X_7$ receptor may be present within the dog.

Our studies confirm that the magnitude of the effect of ATP on cation permeability in canine erythrocytes is at least 20 times greater than that observed in human erythrocytes. Many features of this ATP-induced cation permeability in canine erythrocytes were characteristic of functional $P2X_7$ receptors, and the presence of these receptors was directly shown by immunocytochemistry and immunoblotting. Finally, we demonstrate that overnight incubation with ATP or BzATP induces PS exposure in the majority of canine erythrocytes, with 17% of cells on average undergoing hemolysis. The ATP- or BzATP-induced PS exposure on canine erythrocytes was at least five times greater than that of human erythrocytes, and hemolysis of human erythrocytes was negligible.

Address for reprint requests and other correspondence: R. Sluyter, Dept. of Medicine, Univ. of Sydney, Level 5 South Block, Nepean Hospital, Penrith, New South Wales, Australia (e-mail: rons@med.usyd.edu.au).

The costs of publication of this article were defrayed in part by the payment of page charges. The article must therefore be hereby marked "*advertisement*" in accordance with 18 U.S.C. Section 1734 solely to indicate this fact.

MATERIALS AND METHODS

Reagents. BSA, D-glucose, glycerol gelatin mounting medium, saponin, ATP, BzATP, ATPγS, ADP, AMP, adenosine, UTP, ATP-2′,3′-dialdehyde (oxidized ATP, OxATP), Brilliant blue G (BBG), DMSO, Drabkin's reagent, EDTA, dithiothreitol, rabbit anti-actin antibody, and other general reagent-grade chemicals were obtained from Sigma (St. Louis, MO). 2MeSATP was acquired from Tocris Biosciences (Ellisville, MO). KN-62 was obtained from Biomol Research Laboratories (Plymouth Meeting, PA). Brij 35 was obtained from Merck (Darmstadt, Germany). H_2O_2 was acquired from Fronine Laboratory Supplies (Riverstone, New South Wales, Australia). HEPES, normal horse serum (NHS), and NuPAGE SDS running and transfer buffers were obtained from Invitrogen (Carlsbad, CA). Ficoll-Paque PLUS was obtained from GE Healthcare Biosciences (Uppsala, Sweden). Rubidium-86 ($^{86}Rb^+$), SOLVABLE tissue solubilizer, and Ultima Gold were acquired from PerkinElmer Life Sciences (Boston, MA). [*Methyl*-^{14}C]choline-Cl was obtained from GE Healthcare UK (Little Chalfont, UK). Di-*n*-butyl phthalate and di-isooctyl phthalate (BDH Chemicals, Poole, UK) were blended 80:20 (vol/vol) to give an oil mixture of density 1.03 g/ml. Sheep polyclonal antibody raised against an extracellular epitope of human P2X$_7$ was kindly provided by Dr. Julian A. Barden (University of Sydney, Sydney, New South Wales, Australia) (61). This antibody binds P2X$_7$-transfected but not nontransfected HEK-293 cells as assessed by confocal microscopy (61), as well as a band at the predicted 75-kDa region in P2X$_7$-transfected but not nontransfected HEK-293 cells as determined by Western blotting (20). Cy3-conjugated donkey anti-sheep IgG antibody was obtained from Jackson ImmunoResearch (West Grove, PA). FITC-conjugated murine anti-human CD14 MAb (clone TUK4) and horseradish peroxidase-conjugated rabbit anti-sheep Ig antibody were obtained from Dako (Carpinteria, CA). Horseradish peroxidase-conjugated goat anti-rabbit Ig antibody and SuperSignal West Pico chemiluminescent substrate were acquired from Pierce (Rockford, IL). Phenylmethylsulfonyl fluoride and annexin V-FLUOS were obtained from Roche Diagnostics (Pensberg, Germany).

Erythrocytes and mononuclear cells. The study was approved by the Westmead Hospital Animal Ethics Committee (Westmead, New South Wales, Australia) and the Sydney West Area Health Service Human Ethics Committee (Penrith, New South Wales, Australia). Peripheral blood was collected in heparin-containing vacutainer tubes from four adult English springer spaniels, as well as from five healthy human volunteers. Blood was centrifuged at 580 *g* for 15 min, the plasma and platelets were discarded, and leukocytes and the upper 10% of erythrocytes were collected to obtain buffy coats. The remaining erythrocytes were washed twice in NaCl medium (147.5 mM NaCl, 2.5 mM KCl, 5 mM D-glucose, 0.1% BSA, and 20 mM HEPES, pH 7.5) at 450 *g* for 5 min. To isolate mononuclear cells, buffy coats were diluted in five volumes of NaCl medium, underlaid with Ficoll-Paque PLUS, and centrifuged at 580 *g* for 30 min. Isolated mononuclear cells were washed in NaCl medium at 450 *g* for 10 min.

Immunofluorescence staining and confocal microscopy. Erythrocytes were resuspended in NaCl medium (5×10^7 cells/ml), and 20 μl were smeared onto glass slides, air-dried for 30 min, and fixed with acetone-methanol for 2 min. The slides were washed four times over 10 min with phosphate-buffered saline (PBS; pH 7.2) and blocked with PBS-20% NHS-0.1% BSA for 20 min before incubation for 45 min with anti-P2X$_7$ antibody diluted in PBS-0.2% NHS. The slides were washed three times over 30 min with PBS and incubated for 45 min with Cy3-conjugated secondary antibody diluted in PBS-0.2% NHS. The slides were again washed before being embedded in glycerol gelatin mounting medium. Cells were visualized using a Leica Microsystems (Wetzlar, Germany) laser scanning confocal microscope as described previously (23).

Immunoblotting. Hemoglobin (Hb)-free ghost membranes were prepared as previously described (9) using 20 mM phosphate buffer (pH 7.4) containing 1 mM EDTA and 0.2 mM phenylmethylsulfonyl fluoride. Protein concentrations were determined using the DC protein assay (Bio-Rad, Hercules, CA) with BSA as a standard. Proteins of ghost membranes (20 μg/well) were separated under reducing conditions (100 mM dithiothreitol) using 4–12% gradient NuPAGE Novex Bis-Tris mini gels (Invitrogen) and transferred to nitrocellulose membranes (Bio-Rad) using NuPAGE transfer buffer. Nitrocellulose membranes were blocked overnight at 4°C with 5% skim milk powder in Tris-buffered saline containing Tween 20 (TBST; 250 mM NaCl, 50 mM Tris, and 0.2% Tween 20, pH 7.5) and then incubated for 2 h at room temperature with either anti-P2X$_7$ or anti-actin antibody diluted in TBST containing 5% skim milk powder. Membranes were washed three times over 30 min with TBST and then incubated for 1 h at room temperature with either horseradish peroxidase-conjugated anti-sheep or anti-rabbit Ig antibody, respectively, diluted in TBST containing 5% skim milk powder. Membranes were washed, incubated with chemiluminescent substrate, and visualized using a Gel Doc system and Quantity One software (Bio-Rad).

$^{86}Rb^+$ efflux measurements. Erythrocytes were loaded with $^{86}Rb^+$ (5 μCi/ml) at a hematocrit of 40% in NaCl medium for 4 h at 37°C. Cells were then washed three times with ice-cold NaCl medium at 4°C (1,800 *g* for 3 min) and resuspended in either NaCl medium or KCl medium (150 mM KCl, 5 mM D-glucose, 0.1% BSA, and 20 mM HEPES, pH 7.5) at a final hematocrit of 5%. $^{86}Rb^+$-loaded erythrocyte suspensions were incubated in the absence or presence of nucleotide for up to 40 min at 37°C. At 0, 2, 12, 20, or 40 min, 1-ml samples were overlaid on 300 μl of phthalate oil mixture and centrifuged at 8,000 *g* for 30 s. For studies using the P2X$_7$ antagonist OxATP (40), $^{86}Rb^+$-loaded erythrocytes in NaCl medium were preincubated in the absence or presence of 300 μM OxATP for 60 min at 37°C, washed once with NaCl medium, and resuspended in NaCl medium before incubation in the absence or presence of ATP for 12 min. For studies using the P2X$_7$ antagonists KN-62 (17) and BBG (28), $^{86}Rb^+$-loaded erythrocytes resuspended in NaCl medium were preincubated in the presence or absence of 1 μM KN-62, 1 μM BBG, or an equal volume of DMSO vehicle for 5 min at 37°C before incubation in the absence or presence of ATP for 12 min. The level of radioactivity in cell lysates (lysed with an equal volume of 0.4% saponin) and supernatants was measured using a Wallac (Turku, Finland) 1480 Wizard 3" automatic gamma counter. Hemolysis (Hb release) was determined spectrophotometrically on cell-free supernatants with Drabkin's reagent (containing 0.015% Brig 35) according to the manufacturer's instructions.

Choline$^+$ uptake measurements. Erythrocytes were washed once with choline-Cl medium (150 mM choline-Cl, 5 mM D-glucose, 0.1% BSA, 20 mM HEPES, pH 7.5). Erythrocyte suspensions (2 ml) at a final hematocrit of 5% in choline Cl medium containing [*methyl*-^{14}C]choline$^+$ (1 μCi/ml) were incubated in the absence or presence of 1 mM ATP for up to 40 min at 37°C. At 2, 20, or 40 min, cells were washed three times with ice-cold isotonic saline containing 1 mM choline-Cl (1,800 *g* for 60 s). To determine the level of [^{14}C]choline$^+$ uptake, 50-μl aliquots of erythrocyte pellets were incubated with 1 ml of SOLVABLE tissue solubilizer for 1 h at 60°C, followed by incubation with 100 μl of 100 mM EDTA and 500 μl of 30% H_2O_2 for 30 min at room temperature and then for a further 30 min at 60°C before the addition of 10 ml of Ultima Gold. The level of radioactivity was measured using a Packard (Meriden, CT) Tri-Carb 2100TR liquid scintillation analyzer. The Hb content of erythrocyte pellets (50 μl) was measured spectrophotometrically using Drabkin's reagent. The Hb content was used to determine the level of choline$^+$ uptake per milliliter of canine and human erythrocytes based on mean cell Hb concentrations of 5.4 and 5.2 μmol Hb/ml, respectively.

Ethidium$^+$ uptake measurements. Mononuclear cells were prelabeled with FITC-conjugated anti-CD14 MAb and resuspended in 1 ml of KCl medium at 37°C. At 0 s, 25 μM ethidium$^+$ was added, followed 40 s later by the addition of ATP as indicated. In some experiments, cells were preincubated for 5 min at 37°C in the presence of KN-62 or an equal volume of DMSO vehicle. Data were collected

using a Becton Dickinson (San Jose, CA) FACScalibur flow cytometer over 6 min at 37°C with constant stirring using a Cytek (Fremont, CA) Time Zero module. The linear mean channel of ethidium$^+$ fluorescence intensity for each gated population over successive 5-s intervals was analyzed using WinMDI 2.8 software developed by Joseph Trotter (http://www.scripps.edu) and plotted against time. Nucleotide-induced ethidium$^+$ uptake was quantified as the difference in arbitrary units of area under the uptake curves in the presence and absence of nucleotide in the first 5 min of incubation.

PS exposure assay. Erythrocytes, resuspended in NaCl medium (without BSA) at a final hematocrit of 2%, were added to 96-well U-bottom plates (200 μl/well) and incubated in the absence or presence ATP or BzATP for 24 h at 37°C and 95% air-5% CO_2. Erythrocytes (20 μl) were washed in 2 ml of annexin V-binding buffer (NaCl medium without BSA but containing 5 mM $CaCl_2$) and centrifuged at 450 *g* for 3 min. Erythrocytes were incubated at room temperature with 100 μl annexin V-FLUOS diluted 1:100 in annexin V-binding buffer. After 15 min, 400 μl of annexin V-binding buffer were added, and fluorescence intensity was measured using flow cytometry and analyzed using CellQuest Pro software (Becton Dickinson).

Hb release measurements. Erythrocytes were incubated in the absence or presence of ATP or BzATP as for the PS exposure assay. Plates were then centrifuged (1,800 *g* for 5 min), and 100 μl of cell-free supernatants were stored at −30°C for 2 h. Cells and the remaining supernatant in wells were also stored at −30°C for 2 h (cell lysates). The Hb content of supernatants and cell lysates was assayed spectrophotometrically using Drabkin's reagent, and the percent hemolysis was determined.

Statistical analyses. Results are means (SD). Differences between treatments were compared using either the unpaired Student's *t*-test for single comparisons to control samples or ANOVA for multiple comparisons (with Bonferroni post hoc test), using SPSS 14.0 for Windows (SPSS, Chicago, IL) with $P < 0.05$ considered significant.

RESULTS

P2X$_7$ receptors are present on canine erythrocytes. Our laboratory (52) has previously shown, using an anti-human P2X$_7$ antibody and confocal microscopy, that P2X$_7$ receptors are present on human erythrocytes. Using this same procedure, we examined whether P2X$_7$ receptors also are present on canine erythrocytes. Confocal microscopy showed P2X$_7$ to be present on erythrocytes obtained from two different dogs with a punctate pattern of labeling on all cells present (Fig. 1*A* and results not shown). As a positive control and for comparison, erythrocytes from a human subject were examined and showed P2X$_7$ receptor immunoreactivity (Fig. 1*B*). Labeling in the absence of anti-P2X$_7$ antibody was negligible (results not shown).

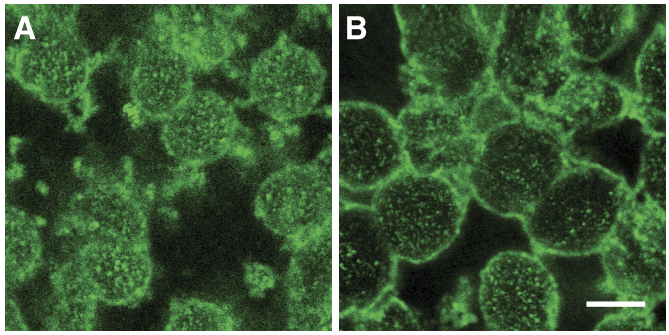

Fig. 1. Expression of P2X$_7$ receptors on canine and human erythrocytes by confocal microscopy. Fixed smears of canine (*A*) or human erythrocytes (*B*) were incubated in the presence (*A* and *B*) or absence (not shown) of sheep anti-P2X$_7$ polyclonal antibody and then with Cy3-conjugated anti-sheep IgG antibody before examination by confocal microscopy. Labeling in the absence of anti-P2X$_7$ antibody was negligible. The calibration bar is 4 μm.

To confirm the presence of P2X$_7$ on canine erythrocytes and to compare its relative expression to P2X$_7$ on human erythrocytes, we performed immunoblotting of erythrocyte ghost membranes isolated from both species. Immunoblotting with the anti-P2X$_7$ antibody revealed the presence of major band at 75 kDa, the predicted size of glycosylated P2X$_7$ (Fig. 2). This 75-kDa band was repeatedly stronger in canine erythrocytes compared with human erythrocytes despite similar levels of actin (Fig. 2). Bands also were evident with the anti-P2X$_7$ antibody at 220 and 72 kDa (Fig. 2), which may represent trimeric P2X$_7$ and differences in P2X$_7$ glycosylation, respectively.

ATP induces $^{86}Rb^+$ efflux from canine erythrocytes. Extracellular ATP induced a near complete loss of $^{42}K^+$ from canine erythrocytes within 40 min (43); therefore, the effect of extracellular ATP on $^{86}Rb^+$ (a surrogate of K^+) efflux in canine erythrocytes was studied as previously carried out for human erythrocytes (52). $^{86}Rb^+$-loaded cells resuspended in NaCl medium were incubated at 37°C with 1 mM ATP for up to 40 min with samples collected at 2, 20, and 40 min. ATP induced a significant increment in $^{86}Rb^+$ efflux from canine erythrocytes at all three time points compared with cells incubated in the absence of ATP for the same length of time ($P = 0.008$, $P < 0.001$, and $P < 0.001$, respectively) (Fig. 3*A*). Comparison of human erythrocytes demonstrates that ATP induced a far smaller increment in $^{86}Rb^+$ efflux (Fig. 3*A*), which only attained significance at longer times of incubation (52).

Similar results were observed when canine erythrocytes were incubated in a KCl medium, with ATP inducing a significant increment in $^{86}Rb^+$ efflux from cells at 2, 20, and 40 min compared with cells incubated in the absence of ATP for the same length of time (all $P < 0.001$) (Fig. 3*B*). In human erythrocytes, ATP induced a small increment in $^{86}Rb^+$ efflux at 2, 20, and 40 min ($P = 0.016$ at 40 min), which was far smaller than that observed with canine erythrocytes (Fig. 3*B*).

P2X$_7$ agonists induce $^{86}Rb^+$ efflux from canine erythrocytes. The dose effect of ATP and the most potent P2X$_7$ agonist, BzATP (16, 57), on $^{86}Rb^+$ efflux from canine erythrocytes was then studied. Cells loaded with $^{86}Rb^+$ were resuspended in NaCl medium and incubated at 37°C with varying concentrations of ATP or BzATP for 12 min. The efflux of $^{86}Rb^+$ from erythrocytes after 12 min of incubation ranged from 2.4% (SD 0.7) in the absence of nucleotide to 61.9% (SD 1.8) with 2 mM ATP and 71.8% (SD 3.4) with 200 μM BzATP (Fig. 4). EC_{50} values of 309 μM (SD 14) for ATP and 7 μM (SD 1) for BzATP were obtained from these dose-response curves, which are comparable to respective EC_{50} values for BzATP-and ATP-induced cation fluxes mediated by recombinant murine, rat, and human P2X$_7$ receptors (7).

In addition to ATP and BzATP, the partial P2X$_7$ agonists (16, 57) 2MeSATP and ATPγS (1 mM) induced a smaller but significant $^{86}Rb^+$ efflux of 16.4% (SD 2.2) ($P = 0.005$) and 14.6% (SD 1.8) ($P = 0.008$), respectively (Fig. 5). Agonists of P1 and other P2 receptors, adenosine, AMP, ADP, and UTP (1 mM), resulted in a release of $^{86}Rb^+$ similar to that of control values (Fig. 5). Thus, for canine erythrocytes, the ability of

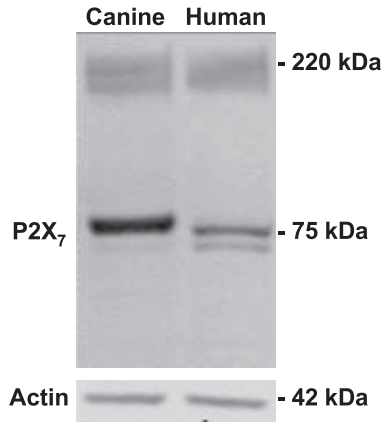

Fig. 2. Expression of P2X$_7$ receptors on canine and human erythrocytes by immunoblotting. Proteins of Hb-free ghost membranes were separated by gel electrophoresis and transferred to nitrocellulose membranes. Nitrocellulose membranes were incubated with anti-P2X$_7$ or anti-actin antibody and then with horseradish peroxidase-conjugated anti-sheep or anti-rabbit Ig antibody, respectively, before visualization with chemiluminescent substrate. Actin served as a loading control. Representative results of 2 experiments are shown.

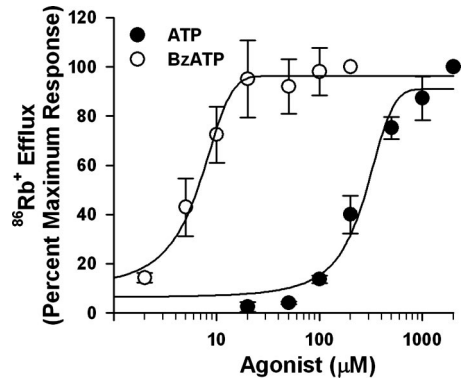

Fig. 4. Dose-response curves for ATP- and 2′(3′)-*O*-(4-benzoylbenzoyl) adenosine 5′-trisphosphate (BzATP)-induced $^{86}Rb^+$ efflux from canine erythrocytes. $^{86}Rb^+$-loaded erythrocytes resuspended in NaCl medium were incubated at 37°C for 12 min in the presence of varying ATP or BzATP concentrations as indicated. $^{86}Rb^+$ release, calculated as the difference in percent release between 0 and 12 min, was used to determine the percentage of maximal response to 2 mM ATP or 200 μM BzATP. Results are means (SD) (n = 3).

nucleotides to induce $^{86}Rb^+$ efflux follows a rank order of BzATP > ATP > 2MeSATP > ATPγS, which is identical to that observed for cation fluxes mediated by rat and human P2X$_7$ receptors (16, 57). UTP, ADP, AMP, and adenosine were ineffective, thus excluding a role for many of the P2Y and adenosine receptors, some of which are found in mammalian and avian erythrocytes (4, 56, 58, 59).

The percent release of Hb after 12 min of incubation with BzATP or ATP was measured using Drabkin's reagent. Hb release in the absence of nucleotide was 1.1% (0.5 SD) (n =3). BzATP but not ATP induced a small but significant release of Hb from erythrocytes: 3.7% (SD 11.7) (P = 0.024) and 2.7% (SD 1.1) (P = 0.084), respectively (n =3). Thus the ATP- and the majority of the BzATP-induced $^{86}Rb^+$ release was a result of efflux rather than hemolysis.

P2X$_7$ antagonists inhibit ATP-induced $^{86}Rb^+$ efflux from canine erythrocytes. To confirm that ATP-induced $^{86}Rb^+$ efflux from canine erythrocytes was mediated by P2X$_7$ activation, we preincubated $^{86}Rb^+$-loaded cells in the absence or presence of OxATP, KN-62, or BBG, antagonists of human, mouse, and rat P2X$_7$ (17, 28, 40), and the ATP-induced $^{86}Rb^+$

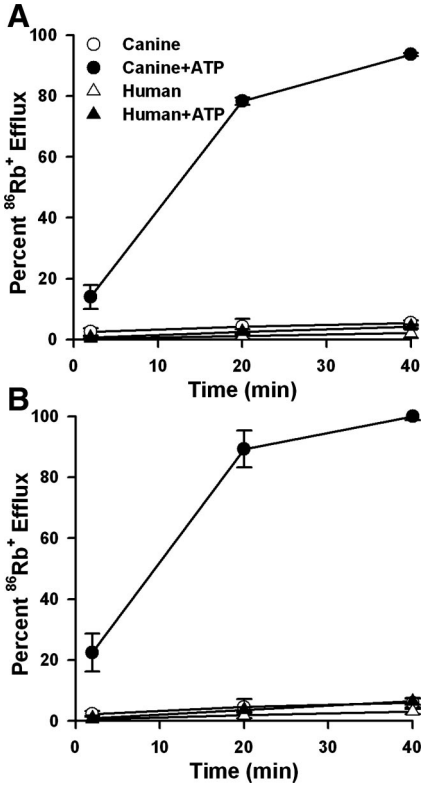

Fig. 3. Time course of ATP-induced $^{86}Rb^+$ efflux from canine and human erythrocytes. $^{86}Rb^+$-loaded canine or human erythrocytes resuspended in NaCl (*A*) or KCl medium (*B*) were incubated at 37°C for up to 40 min in the absence or presence of 1 mM ATP. $^{86}Rb^+$ efflux was calculated as the difference in percent release between 0 and 2, 20, or 40 min. Results are means (SD) (n = 3).

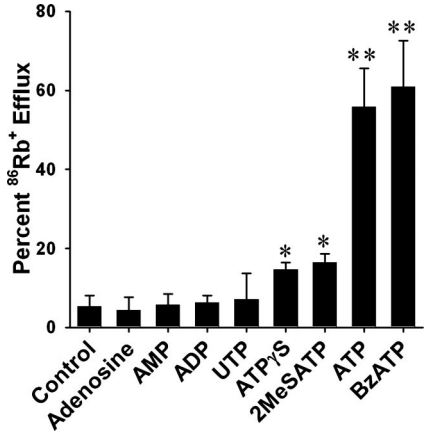

Fig. 5. P2X$_7$ agonists induce $^{86}Rb^+$ efflux from human erythrocytes. $^{86}Rb^+$-loaded erythrocytes resuspended in NaCl medium were incubated at 37°C for 12 min in the absence (control) or presence of 1 mM nucleotide or adenosine (as indicated) except for BzATP (100 μM). $^{86}Rb^+$ efflux was calculated as the difference in percent release between 0 and 60 min. *P < 0.01; **P = 0.001 compared with control. Results are means (SD) from 3 different animals. ATPγS, adenosine 5′-*O*-(3-thiotriphosphate); 2MeSATP, 2-methylthioadenosine 5′-triphosphate.

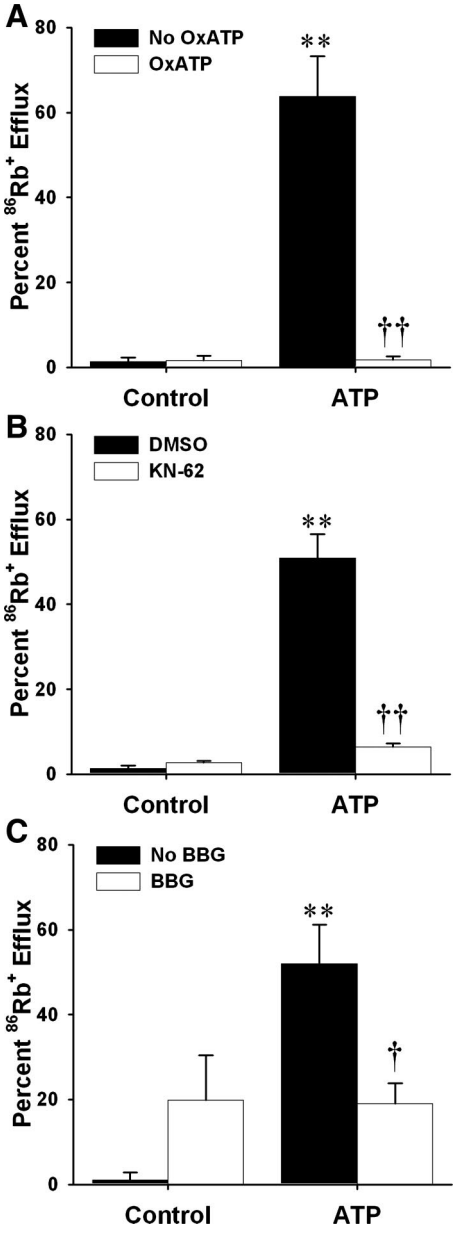

Fig. 6. P2X$_7$ antagonists impair ATP-induced $^{86}Rb^+$ efflux from canine erythrocytes. $^{86}Rb^+$-loaded erythrocytes resuspended in NaCl medium were preincubated at 37°C for 60 min in the absence or presence of 300 μM oxidized ATP (OxATP; *A*) or for 5 min in the absence or presence of DMSO vehicle or 1 μM KN-62 (*B*) or 1 μM Brilliant blue G (BBG; *C*) and then incubated at 37°C for 12 min in the absence (control) or presence of ATP. $^{86}Rb^+$ efflux was calculated as the difference in percent release between 0 and 12 min. *$P < 0.001$ compared with control. †$P < 0.01$; ††$P < 0.001$ compared with corresponding ATP-treated sample. Results are means (SD) ($n = 3$).

effluxes were measured. Incubation with 300 μM OxATP, 1 μM KN-62, or 1 μM BBG significantly inhibited 1 mM ATP-induced $^{86}Rb^+$ efflux by 98.51% (SD 1.4) ($P < 0.001$), 92.7% (SD 3.5) ($P < 0.001$), and 94.2% (SD 5.9) ($P = 0.003$), respectively (Fig. 6). Neither OxATP nor KN-62 altered the basal release of $^{86}Rb^+$ from erythrocytes incubated in the absence of ATP. In contrast, BBG increased the basal release of $^{86}Rb^+$ in the absence of ATP compared with erythrocytes incubated without both BBG and ATP; however, this failed to reach significance ($P = 0.058$).

ATP induces choline$^+$ uptake into canine and human erythrocytes. To determine whether the difference in P2X$_7$ function between canine and human erythrocytes was also apparent with larger, more complex cations and thus directly implicating the P2X$_7$ pore, we measured the ability of ATP to induced choline$^+$ uptake into these cells. Erythrocytes resuspended in 150 mM choline-Cl medium containing [^{14}C]choline$^+$ were incubated at 37°C with 1 mM ATP for up to 40 min with samples collected at 2, 20, and 40 min. ATP induced a significant increment in choline$^+$ uptake into canine erythrocytes at all three time points compared with cells incubated in the absence of ATP for the same length of time (all $P < 0.001$) (Fig. 7). Comparison of human erythrocytes showed that ATP induced a far smaller increment in choline$^+$ uptake (Fig. 7), which only reached significance at 40 min ($P = 0.043$).

ATP induces ethidium$^+$ uptake into canine monocytes. Collectively, the above data indicate that functional P2X$_7$ receptors are expressed on canine erythrocytes and that P2X$_7$ function in this cell type is at least 20 times higher than in human erythrocytes. Therefore, to determine whether this difference was limited to canine erythrocyte P2X$_7$ or canine P2X$_7$ per se, we compared the ability of ATP to induce ethidium$^+$ uptake in canine monocytes with that in CD14$^+$ human monocytes. Mononuclear cells isolated from dogs or humans were prelabeled with FITC-conjugated anti-human CD14 MAb (clone TUK4), and the ability of 1 mM ATP to induce ethidium$^+$ uptake over 5 min was measured using time-resolved flow cytometry as described previously (30). The anti-human CD14 MAb binds to canine monocytes, but not canine lymphocytes or granulocytes (26), as well as to human monocytes. ATP induced the uptake of ethidium$^+$ into CD14$^+$ canine monocytes with a mean uptake of 11,251 arbitrary units of area under the curve (SD 1,199) (Fig. 8). The ATP-induced uptake of ethidium$^+$ into CD14$^+$ human monocytes was on average three times higher ($P < 0.001$) than that of canine monocytes, with a mean uptake of 36,177 arbitrary units of area under the

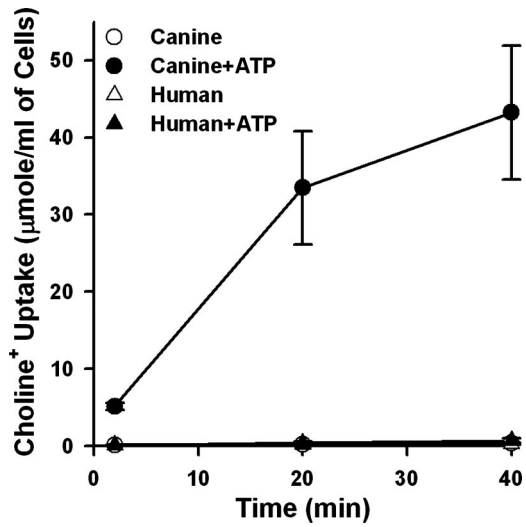

Fig. 7. ATP induces choline$^+$ uptake into canine and human erythrocytes. Canine or human erythrocytes resuspended in 150 mM choline-Cl medium containing [*methyl*-^{14}C]choline$^+$ (1 μCi/ml) were incubated at 37°C for up to 40 min in the absence or presence of 1 mM ATP. The level of choline$^+$ uptake at each time point was determined as μmol of choline$^+$ per milliliter of cells. Results are means (SD) ($n = 4$).

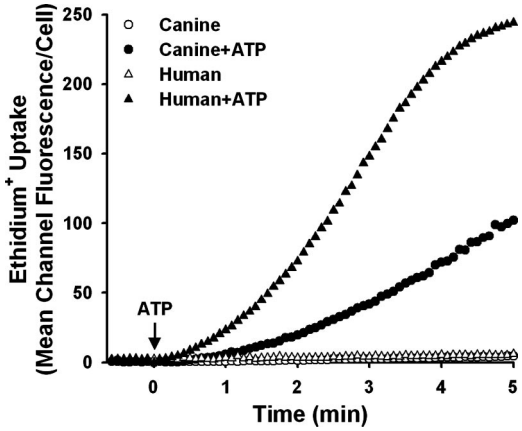

Fig. 8. ATP induces ethidium$^+$ uptake into canine and human monocytes. Canine or human mononuclear cells were prelabeled with FITC-CD14 MAb and resuspended in KCl medium at 37°C. Ethidium$^+$ (25 μM) was added, followed 40 s later by the addition of 1 mM ATP (arrow). The mean channel of cell-associated fluorescence was measured using time-resolved flow cytometry for CD14$^+$ monocytes incubated in the absence or presence of ATP. Representative results from 3 experiments are shown.

curve (SD 2,264) (Fig. 8). The uptake of ethidium$^+$ into CD14$^+$ canine and human monocytes in the absence of ATP was minimal (Fig. 8).

The effect of the P2X$_7$ antagonist KN-62 on the ATP-induced ethidium$^+$ uptake into CD14$^+$ canine monocytes was measured. ATP induced ethidium$^+$ uptake into CD14$^+$ canine monocytes preincubated with DMSO vehicle with a mean uptake of 18,925 arbitrary units of area under the curve (SD 362) (Fig. 9). Preincubation of cells with 1 μM KN-62 significantly inhibited the ATP-induced ethidium$^+$ uptake by 89.3% (SD 2.0) (Fig. 9). Collectively, these results demonstrate that ATP can induce the uptake of ethidium$^+$ into CD14$^+$ canine monocytes via activation of the P2X$_7$ receptors and that canine monocytes do not share the very high P2X$_7$ function of erythrocytes from this species.

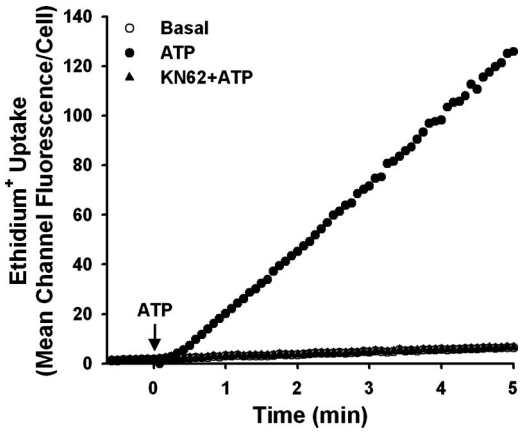

Fig. 9. A P2X$_7$ antagonist impairs ATP-induced ethidium$^+$ uptake into canine monocytes. Canine mononuclear cells were prelabeled with FITC-CD14 MAb and resuspended in KCl medium at 37°C. Cells were preincubated at 37°C for 5 min in the absence or presence of DMSO vehicle or 1 μM KN-62. Ethidium$^+$ (25 μM) was then added, followed 40 s later by the addition of 1 mM ATP (arrow). The mean channel of cell-associated fluorescence was measured using time-resolved flow cytometry for CD14$^+$ monocytes incubated in the absence (basal) or presence of ATP. Representative results from 3 experiments are shown.

ATP induces PS exposure and hemolysis in canine erythrocytes. We have recently shown that P2X$_7$ activation induces PS exposure in human erythrocytes (54). Therefore, we compared ATP- or BzATP-induced PS exposure in canine and human erythrocytes. Erythrocytes were incubated with 1 mM ATP or 100 μM BzATP for 24 h, and PS exposure was measured as annexin V-FLUOS binding. Annexin V-FLUOS binding on canine erythrocytes following incubation in the absence of nucleotide was 1.0% (SD 0.6) (Fig. 10). Both ATP and BzATP induced massive PS exposure with 88.6% (SD 8.7) and 98.8% (SD 1.1) of erythrocytes binding annexin V-FLUOS, respectively (both $P < 0.001$) (Fig. 10). Similar to our previous findings (54), ATP and BzATP induced a much smaller PS exposure in human erythrocytes with 13.7% (SD 5.8) and 21.3% (SD 7.0) of cells binding annexin V-FLUOS, respectively (Fig. 10). Annexin V-FLUOS binding on human erythrocytes following incubation in the absence of nucleotide (4.9%, SD 1.1) was significantly lower in response to either agonist (both $P < 0.001$) (Fig. 10).

In our previous study (54), overnight incubation with either ATP or BzATP failed to induce significant hemolysis of human erythrocytes; however, it became apparent during the PS exposure assays that both ATP and BzATP caused hemolysis of some canine erythrocytes. Spectrophotometric measurements of Hb using Drabkin's reagent demonstrated that 24-h incubation with ATP or BzATP induced significant hemolysis of canine erythrocytes with a Hb release of 16.4% (SD 3.6) and 17.2% (SD 4.4), respectively ($n = 6$) (both $P < 0.001$). In contrast, Hb release from canine erythrocytes incubated in the absence of nucleotide was 1.0% (0.6) ($n = 6$). Again as previously observed (54), Hb release from human erythrocytes following 24-h treatment with ATP and BzATP was negligible with values of 0.6% (0.5) and 0.8% (0.7) respectively, which were not significantly different from control values of 0.5% (0.5) ($n = 6$) ($P = 0.759$ and 0.343, respectively).

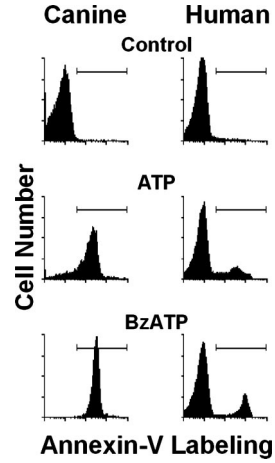

Fig. 10. Flow cytometric profiles of phosphatidylserine (PS) exposure on canine and human erythrocytes incubated with P2X$_7$ agonists. Canine or human erythrocytes resuspended in NaCl medium (without BSA) were incubated at 37°C and 95% air-5% CO_2 for 24 h in the absence (control) or presence of 1 mM ATP or 100 μM BzATP. Cells were labeled with annexin V-FLUOS, and fluorescence intensity was measured using flow cytometry. The percentage of erythrocytes binding annexin V-FLUOS was calculated from the marker region as shown. Representative results from 6 experiments are shown.

DISCUSSION

Over 30 years ago, Parker and Snow demonstrated that extracellular ATP but not other nucleotides could increase the permeability of canine erythrocytes to small cations (43), and this effect was confirmed by other investigators (11, 49). Although the molecular target of ATP was never identified in this process, the discovery of the P2X receptor family (42), and in particular the discovery of the P2X$_7$ receptor on human erythrocytes (52), suggests the involvement of the canine homolog of P2X$_7$. The present data demonstrate that immunoreactive P2X$_7$ receptors are present in canine erythrocytes and that their function, as assessed using cation fluxes, is at least 20 times greater than that of human erythrocytes. Immunocytochemistry and immunoblotting with an anti-human P2X$_7$ polyclonal antibody (61) demonstrated P2X$_7$ on canine erythrocytes (Figs. 1 and 2). This antibody recognizes a 17-amino acid epitope within the extracellular domain of the human P2X$_7$ receptor (KVKGIAEVKEEIVENGVK), which differs by four residues (underlined) from the homologous epitope in the canine P2X$_7$ receptor (KVKGTAEVKMEILENGIK) as reported by the Canine Genome Project (GenBank accession no. XM_534669) (36). The effect of extracellular ATP on $^{86}Rb^+$ (K^+) efflux from canine erythrocytes also was examined as previously described for human erythrocytes (52). ATP increased the $^{86}Rb^+$ efflux from canine erythrocytes to an extent similar (Fig. 3) to that reported previously (43, 49), with cation equilibration reached by 40 min. The effect of ATP and other nucleotides was characteristic of P2X$_7$ receptors found in other species. First, BzATP was more potent than ATP in causing $^{86}Rb^+$ efflux from canine erythrocytes with EC_{50} values of 7 and 309 μM, respectively (Fig. 4), values that are similar to those for recombinant human and rodent P2X$_7$ receptors (7, 46, 57). Second, the rank order of agonist potency (BzATP > ATP > 2MeSATP > ATPγS) (Fig. 5) was typical of other mammalian P2X$_7$ receptors (16, 57). Third, ATP-induced $^{86}Rb^+$ efflux was inhibited by OxATP, KN-62, and BBG (Fig. 6), antagonists of human and/or rodent P2X$_7$ receptors (17, 28, 40). Fourth, P2X$_7$ activation induces the uptake of choline$^+$ into murine macrophages (10) and human B lymphocytes (15), and we similarly observed that ATP induced choline$^+$ uptake into canine erythrocytes (Fig. 7). Finally, both BzATP and ATP induced PS exposure (Fig. 10) and hemolysis (cytolysis) in canine erythrocytes, two well-known downstream events of P2X$_7$ activation in leukocytes (8).

Comparison of P2X$_7$ function in canine and human erythrocytes in this study, as well as between previous studies (43, 52), demonstrates that P2X$_7$ function as determined by ATP-induced $^{86}Rb^+$ efflux and choline$^+$ uptake is at least 20 times greater in canine erythrocytes than in human erythrocytes (Figs. 3 and 7). Moreover, ATP and BzATP induce at least five times the amount of PS externalization in canine erythrocytes compared with human erythrocytes (Fig. 10), and these agonists also induce significant hemolysis of canine but not human erythrocytes. The level of ATP- and BzATP-induced PS exposure in human erythrocytes, as well as the absence of nucleotide-induced hemolysis, was similar to that previously reported (54). The differences between the two species in regard to P2X$_7$ function is specific to erythrocytes and is not due to canine P2X$_7$ per se, since P2X$_7$ function in canine monocytes, measured as ATP-induced ethidium$^+$ uptake, was three times lower than the P2X$_7$ function in human monocytes tested in this study (Fig. 8) and within the lower end of the range for wild-type human monocytes obtained in previous studies in our laboratory (21, 53). Immunoblotting with an anti-human P2X$_7$ antibody revealed a more intense band at 75 kDa, the predicted size of P2X$_7$, in canine erythrocytes compared with human erythrocytes despite equal protein loading and similar levels of actin (Fig. 2). This indicates that a difference in P2X$_7$ expression is the most likely cause for differences in P2X$_7$ function between canine and human erythrocytes. We cannot, however, exclude differences in expression or function of secondary messengers and/or molecules thought to be responsible for P2X$_7$ pore formation (13). In this regard, pannexin-1, which is present in human erythrocytes (37), was recently implicated as the pore-forming unit of the P2X$_7$ receptor (38, 45); thus relatively higher levels of pannexin-1 in canine erythrocytes may also explain the high P2X$_7$ function in this cell type. Differences in levels of P2X$_7$, pannexin-1, or secondary messengers in canine and human erythrocytes may be due to variations in the proteolytic systems responsible for maturation-associated degradation in reticulocytes (2), which exist in both canine and human red blood cells (25, 47).

It is unlikely that variations in protein structure account for the differences observed between canine and human erythrocyte P2X$_7$ function. Comparison between the protein sequences for the canine (GenBank accession no. XM_534669) and human P2X$_7$ receptors (GenBank accession no. Y09561) revealed an overall sequence homology of 85%.[1] Canine P2X$_7$, like human P2X$_7$, comprises 595 amino acids, although an additional residue (asparagine at position 282)[2] is found in the extracellular loop in close proximity to the putative ATP-binding site (20, 48), whereas a valine residue (position 538) is absent from the intracellular carboxyl terminus. The canine P2X$_7$ receptor contains several conserved residues or motifs important in the expression or function of human and rodent P2X receptors. Residues (K64, F198/T199, N293/F/R295 and R308) important in the binding of ATP to P2X receptors (20, 48) are conserved within canine P2X$_7$. Also, cysteine residues within the extracellular domain and an intracellular motif (Y384/X/X/X/K388) are both important in the trafficking of P2X receptors (6, 12). In addition, the canine P2X$_7$ receptor, like other mammalian P2X$_7$ receptors, contains a putative phosphorylation site at Y344 (32) and a threonine-serine cluster (T358/Y/S/S361) (14), both of which regulate function (32, 51). Finally, the canine P2X$_7$ retains conserved residues at those polymorphic sites known to alter P2X$_7$ function or expression in humans (20, 21, 51, 53, 61) and mice (1).

ATP-induced $^{86}Rb^+$ efflux from canine erythrocytes was inhibited by >90% by three commonly used inhibitors of mammalian P2X$_7$ receptors, OxATP, KN-62, and BBG (Fig. 6). OxATP at concentrations of 100 and 300 μM was originally shown to completely block native P2X$_7$ in murine macrophages (40) and human lymphocytes (60), respectively. Subsequently, OxATP was also shown to inhibit recombinant

[1] Comparison was made using Basic Local Alignment Search Tool (BLAST) (http://www.ncbi.nlm.nih.gov/BLAST/Blast.cgi).

[2] Numbering of amino acid positions cited in this and subsequent instances are based on the canine P2X$_7$ receptor sequence (GenBank accession no. XM_534669).

human, murine, and rat $P2X_7$ receptors (22). KN-62 at 100 nM can completely block native $P2X_7$ in human lymphocytes (17), whereas 10-fold higher concentrations are required to completely inhibit recombinant and native murine $P2X_7$ (7, 22, 50). In contrast, several studies have repeatedly shown that KN-62 is a poor inhibitor of the rat $P2X_7$ receptor (7, 22, 24). BBG blocks both rat and murine $P2X_7$ with about 10-fold greater efficacy than human $P2X_7$, completely blocking the receptor at concentrations of 100 nM (22, 28). In our studies, 1 μM BBG caused a small amount of nonspecific lysis of canine erythrocytes, which was not apparent at 100 nM; however, at this concentration BBG only blocked ATP-induced $^{86}Rb^+$ efflux by ~50% (results not shown). In summary, although we did not determine the relative potency of OxATP, KN-62, and BBG against the canine $P2X_7$ receptor, our results demonstrate that these antagonists would be useful in establishing the presence of native $P2X_7$ receptors in other canine cell types.

The physiological significance of $P2X_7$ on canine erythrocytes, as well as on human erythrocytes, is currently unknown. We have previously shown that $P2X_7$ activation induces PS exposure on human erythrocytes (54), whereas in this study 24-h incubation of canine erythrocytes with either ATP or BzATP also induced PS exposure (Fig. 10), with ~17% of canine erythrocytes on average undergoing hemolysis. PS exposure on erythrocytes can lead to their recognition and removal by splenic macrophages and Kupffer cells, as well as adherence to endothelial cells (3, 34). Thus $P2X_7$ activation may play a role in the destruction of erythrocytes after their approximate 120-day life spans, a hypothesis consistent with the $P2X_7$-mediated hemolysis of canine erythrocytes. Alternatively, $P2X_7$ activation may lead to PS-exposing erythrocytes adhering to endothelium and contributing to vaso-occlusion (3, 34). Conversely, erythrocyte $P2X_7$ may play a role in vasodilation or antithrombotic functions, given that a recent study demonstrated that $P2X_7$ activation induces the release of epoxyeicosatrienoic acids from rat erythrocytes (27). $P2X_7$ activation also may play a role in vascular dysfunction, since hydrolysis of PS-exposing erythrocytes by secretory phospholipase A_2 can generate lysophosphatidic acid, which can increase loss of vascular integrity and eventual tissue damage (41). Finally, pannexin-1 is thought to mediate ATP release from erythrocytes (37); thus, if $P2X_7$ couples to pannexin-1 in these cells, it may trigger the release of ATP, which in turn may activate purinergic receptors on erythrocytes and endothelium. Further studies are required to determine the physiological role of $P2X_7$ receptors in erythrocytes and whether differences in $P2X_7$ function between species is of physiological significance, as well as whether $P2X_7$ couples to pannexin-1 in erythrocytes.

Canine erythrocytes also may express $P2Y_1$ and $P2Y_{13}$ receptors, as found in human erythrocytes (58, 59). $P2Y_1$ receptor activation is involved in the induction of an osmolyte permeability in malaria-infected and oxidized erythrocytes (58), whereas ADP activation of $P2Y_{13}$ receptors impairs ATP release from erythrocytes (59). Thus the current physiological roles of these P2Y receptors and the $P2X_7$ receptor in erythrocytes appear quite distinct; however, the possibility remains that these receptors may interact. Activation of erythrocyte $P2Y_1$ and possibly $P2X_7$ receptors by autocrine ATP may be limited by $P2Y_{13}$ receptor signaling induced by ADP resulting from the hydrolysis of ATP. Moreover, activation of erythrocyte P2Y receptors may inhibit $P2X_7$ receptors in these cells similarly to that observed with P2Y receptors and $P2X_3$ receptors in dorsal root ganglion neurons (18) and transfected cell systems (19). Further studies investigating whether canine erythrocytes express other purinergic receptors and the potential interactions between these receptors in erythrocytes are warranted.

In conclusion, we have demonstrated that canine erythrocytes express functional $P2X_7$ receptors and that this receptor is responsible for the long-known ability of extracellular ATP to mediate large increases in cation permeability in these cells. Identification of the canine $P2X_7$ receptor may help in providing a better understanding of $P2X_7$ receptor expression and function and of cation transport in erythrocytes.

GRANTS

This work was supported by the National Health and Medical Research Council of Australia, Cure Cancer Australia, and Nepean Medical Research Foundation.

REFERENCES

1. **Adriouch S, Dox C, Welge V, Seman M, Koch-Nolte F, Haag F.** Cutting edge: a natural P451L mutation in the cytoplasmic domain impairs the function of the mouse $P2X_7$ receptor. *J Immunol* 169: 4108–4112, 2002.
2. **Boches FS, Golderberg AL.** Role for the adenosine triphosphate-dependent proteolytic pathway in reticulocyte maturation. *Science* 215: 978–980, 1982.
3. **Bosman GJ, Willekens FL, Werre JM.** Erythrocyte aging: a more than superficial resemblance to apoptosis? *Cell Physiol Biochem* 16: 1–8, 2005.
4. **Boyer JL, Downes CP, Harden TK.** Kinetics of activation of phospholipase C by P_{2Y} purinergic receptor agonists and guanine nucleotides. *J Biol Chem* 264: 884–890, 1989.
5. **Burnstock G, Knight GE.** Cellular distribution and functions of P2 receptor subtypes in different systems. *Int Rev Cytol* 240: 31–304, 2004.
6. **Chaumont S, Jiang LH, Penna A, North RA, Rassendren F.** Identification of a trafficking motif involved in the stabilization and polarization of P2X receptors. *J Biol Chem* 279: 29628–29638, 2004.
7. **Chessell IP, Simon J, Hibell AD, Michel AD, Barnard EA, Humphrey PP.** Cloning and functional characterisation of the mouse $P2X_7$ receptor. *FEBS Lett* 439: 26–30, 1998.
8. **Di Virgilio F, Chiozzi P, Falzoni S, Ferrari D, Sanz JM, Venketaraman V, Baricordi OR.** Cytolytic P2X purinoceptors. *Cell Death Differ* 5: 191–199, 1998.
9. **Dodge JT, Mitchell C, Hanahan DJ.** The preparation and chemical characteristics of hemoglobin-free ghosts of human erythrocytes. *Arch Biochem Biophys* 100: 119–130, 1963.
10. **El-Moatassim C, Dubyak GR.** Dissociation of the pore-forming and phospholipase D activities stimulated via P_{2Z} purinergic receptors in BAC1.2F5 macrophages: product inhibition of phospholipase D enzyme activity. *J Biol Chem* 268: 15571–15578, 1993.
11. **Elford BC.** Independent routes for Na transport across dog red cell membranes. *Nature* 256: 580–582, 1976.
12. **Ennion S, Evans RJ.** Conserved cysteine residues in the extracellular loop of the human $P2X_1$ receptor form disulfide bonds and are involved in receptor trafficking to the cell surface. *Mol Pharmacol* 61: 303–311, 2000.
13. **Faria RX, Defarias FP, Alves LA.** Are second messengers crucial for opening the pore associated with P2X7 receptor? *Am J Physiol Cell Physiol* 288: C260–C271, 2005.
14. **Feng YH, Wang L, Wang Q, Li X, Zeng R, Gorodeski GI.** ATP stimulates GRK-3 phosphorylation and β-arrestin-2-dependent internalization of $P2X_7$ receptor. *Am J Physiol Cell Physiol* 288: C1342–C1356, 2005.
15. **Fernando KC, Gargett CE, Wiley JS.** Activation of the $P2Z/P2X_7$ receptor in human lymphocytes produces a delayed permeability lesion: Involvement of phospholipase D. *Arch Biochem Biophys* 362: 197–202, 1999.
16. **Gargett CE, Cornish JE, Wiley JS.** ATP, a partial agonist for the P2Z receptor of human lymphocytes. *Br J Pharmacol* 122: 911–917, 1997.
17. **Gargett CE, Wiley JS.** The isoquinoline derivative KN-62 a potent antagonist of the P2Z-receptor of human lymphocytes. *Br J Pharmacol* 120: 1483–1490, 1997.

18. **Gerevich Z, Muller C, Illes P.** Metabotropic P2Y$_1$ receptors inhibit P2X$_3$ receptor-channels in rat dorsal root ganglion neurons. *Eur J Pharmacol* 521: 34–38, 2005.
19. **Gerevich Z, Zadori Z, Muller C, Wirkner K, Schroder W, Rubini P, Illes P.** Metabotropic P2Y receptors inhibit P2X$_3$ receptor-channels via G protein-dependent facilitation of their desensitization. *Br J Pharmacol* 151: 226–236, 2007.
20. **Gu BJ, Sluyter R, Skarratt KK, Shemon AN, Dao-Ung LP, Fuller SJ, Barden JA, Clarke AL, Petrou S, Wiley JS.** An Arg^{307} to Gln polymorphism within the ATP binding site causes loss of function of the human P2X$_7$ receptor. *J Biol Chem* 279: 31287–31295, 2004.
21. **Gu BJ, Zhang WY, Worthington RA, Sluyter R, Dao-Ung P, Petrou S, Barden JA, Wiley JS.** A Glu-496 to Ala polymorphism leads to loss of function of the human P2X$_7$ receptor. *J Biol Chem* 276: 11135–11142, 2001.
22. **Hibell AD, Thompson KM, Xing M, Humphrey PP, Michel AD.** Complexities of measuring antagonist potency at P2X$_7$ receptor orthologs. *J Pharmacol Exp Ther* 296: 947–957, 2001.
23. **Hughes WE, Elgundi Z, Huang P, Frohman MA, Biden TJ.** Phospholipase D1 regulates secretagogue-stimulated insulin release in pancreatic β-cells. *J Biol Chem* 279: 27534–27541, 2004.
24. **Humphreys BD, Virginio C, Surprenant A, Rice J, Dubyak GR.** Isoquinolines as antagonists of the P2X$_7$ nucleotide receptor: high selectivity for the human versus rat receptor homologues. *Mol Pharmacol* 54: 22–32, 1998.
25. **Inaba M, Maede Y.** Na,K-ATPase in dog red cells: immunological identification and maturation-associated degradation by the proteolytic system. *J Biol Chem* 261: 16099–16105, 1986.
26. **Jacobsen CN, Aasted B, Broe MK, Petersen JL.** Reactivities of 20 anti-human monoclonal antibodies with leucocytes from ten different animal species. *Vet Immunol Immunopathol* 39: 461–466, 1993.
27. **Jiang H, Zhu AG, Mamczur M, Falck JR, Lerea KM, McGiff JC.** Stimulation of rat erythrocyte P2X$_7$ receptor induces the release of epoxyeicosatrienoic acids. *Br J Pharmacol* 151: 1033–1040, 2007.
28. **Jiang LH, Mackenzie AB, North RA, Surprenant A.** Brilliant blue G selectively blocks ATP-gated rat P2X$_7$ receptors. *Mol Pharmacol* 58: 82–88, 2000.
29. **Jiang LH, Rassendren F, Mackenzie A, Zhang YH, Surprenant A, North RA.** *N*-methyl-D-glucamine and propidium dyes utilize different permeation pathways at rat P2X$_7$ receptors. *Am J Physiol Cell Physiol* 289: C1295–C1302, 2005.
30. **Jursik C, Sluyter R, Georgiou JG, Fuller SJ, Wiley JS, Gu BJ.** A quantitative method for routine measurement of cell surface P2X$_7$ receptor function in leucocyte subsets by two-colour time-resolved flow cytometry. *J Immunol Methods* 325: 67–77, 2007.
31. **Khakh BS, North RA.** P2X receptors as cell-surface ATP sensors in health and disease. *Nature* 442: 527–532, 2006.
32. **Kim M, Jiang LH, Wilson HL, North RA, Surprenant A.** Proteomic and functional evidence for a P2X$_7$ receptor signalling complex. *EMBO J* 20: 6347–6358, 2001.
33. **Kucenas S, Li Z, Cox JA, Egan TM, Voigt MM.** Molecular characterization of the zebrafish P2X receptor subunit gene family. *Neuroscience* 121: 935–945, 2003.
34. **Kuypers FA, De Jong K.** The role of phosphatidylserine in recognition and removal of erythrocytes. *Cell Mol Biol (Noisy-le-grand)* 50: 147–158, 2004.
35. **Lee HK, Ro S, Keef KD, Kim YH, Kim HW, Horowitz B, Sanders KM.** Differential expression of P2X-purinoceptor subtypes in circular and longitudinal muscle of canine colon. *Neurogastroenterol Motil* 17: 575–584, 2005.
36. **Lindblad-Toh K, Wade CM, Mikkelsen TS, Karlsson EK, Jaffe DB, Kamal M, Clamp M, Chang JL, Kulbokas EJ, Zody MC, Mauceli E, Xie X, Breen M, Wayne RK, Ostrander EA, Ponting CP, Galibert F, Smith DR, deJong PJ, Kirkness E, Alvarez P, Biagi T, Brockman W, Butler J, Chin CW, Cook A, Cuff J, Daly MJ, DeCaprio D, Gnerre S, Grabherr M, Kellis M, Kleber M, Bardeleben C, Goodstadt L, Heger A, Hitte C, Kim L, Koepfli KP, Parker HG, Pollinger JP, Searle SMJ, Sutter NB, Thomas R, Webber C, Broad Institute Sequencing Platform, Lander ES.** Genome sequence, comparative analysis and haplotype structure of the domestic dog. *Nature* 438: 803–819, 2005.
37. **Locovei S, Bao L, Dahl G.** Pannexin 1 in erythrocytes: function without a gap. *Proc Natl Acad Sci USA* 103: 7655–7659, 2006.
38. **Locovei S, Scemes E, Qiu F, Spray DC, Dahl G.** Pannexin 1 is part of the pore forming unit of the P2X$_7$ receptor death complex. *FEBS Lett* 581: 483–488, 2007.
39. **Lopez-Castejon G, Young MT, Meseguer J, Surprenant A, Mulero V.** Characterization of ATP-gated P2X$_7$ receptors in fish provides new insights into the mechanism of release of the leaderless cytokine interleukin-1β. *Mol Immunol* 44: 1286–1299, 2006.
40. **Murgia M, Hanau D, Pizzo P, Rippa M, Di Virgilio F.** Oxidized ATP: an irreversible inhibitor of the macrophage purinergic P2Z receptor. *J Biol Chem* 268: 8199–8203, 1993.
41. **Neidlinger NA, Larkin SK, Bhagat A, Victorino GP, Kuypers FA.** Hydrolysis of phosphatidylserine-exposing red blood cells by secretory phospholipase A$_2$ generates lysophosphatidic acid and results in vascular dysfunction. *J Biol Chem* 281: 775–781, 2006.
42. **North RA.** Molecular physiology of P2X receptors. *Physiol Rev* 82: 1013–1067, 2002.
43. **Parker JC, Snow RL.** Influence of external ATP on permeability and metabolism of dog red blood cells. *Am J Physiol* 223: 888–893, 1972.
44. **Paukert M, Hidayat S, Grunder S.** The P2X$_7$ receptor from *Xenopus laevis*: formation of a large pore in *Xenopus* oocytes. *FEBS Lett* 513: 253–258, 2002.
45. **Pelegrin P, Surprenant A.** Pannexin-1 mediates large pore formation and interleukin-1beta release by the ATP-gated P2X$_7$ receptor. *EMBO J* 25: 5071–5082, 2006.
46. **Rassendren F, Buell G, Newbolt A, North RA, Surprenant A.** The permeabilizing ATP receptor, P2X$_7$. Cloning and expression of human cDNA. *J Biol Chem* 272: 5482–5486, 1997.
47. **Rieder RF, Ibrahim A, Etlinger JD.** A soluble adenosine triphosphate-dependent proteolytic system in human peripheral red blood cells. *Blood* 67: 1293–1297, 1986.
48. **Roberts JA, Vial C, Digby HR, Agboh KC, Wen H, Atterbury-Thomas A, Evans RJ.** Molecular properties of P2X receptors. *Pflügers Arch* 452: 486–500, 2006.
49. **Romualdez A, Volpi M, Sha'afi RI.** Effect of exogenous ATP on sodium transport in mammalian red cells. *J Cell Physiol* 87: 297–306, 1976.
50. **Seman M, Adriouch S, Scheuplein F, Krebs C, Freese D, Glowacki G, Deterre P, Haag F, Koch-Nolte F.** NAD-induced T cell death: ADP-ribosylation of cell surface proteins by ART2 activates the cytolytic P2X7 purinoceptor. *Immunity* 19: 571–582, 2003.
51. **Shemon AN, Sluyter R, Fernando SL, Clarke AL, Dao-Ung LP, Skarratt KK, Saunders BM, Tan KS, Gu BJ, Fuller SJ, Britton WJ, Petrou S, Wiley JS.** A Thr^{357} to Ser polymorphism in homozygous and compound heterozygous subjects causes absent or reduced P2X$_7$ function and function impairs ATP-induced mycobacterial killing by macrophages. *J Biol Chem* 281: 2079–2086, 2006.
52. **Sluyter R, Shemon AN, Barden JA, Wiley JS.** Extracellular ATP increases cation fluxes in human erythrocytes by activation of the P2X$_7$ receptor. *J Biol Chem* 279: 44749–44755, 2004.
53. **Sluyter R, Shemon AN, Wiley JS.** Glu^{496} to Ala polymorphism in the P2X$_7$ receptor impairs ATP-induced IL-1β release from human monocytes. *J Immunol* 172: 3399–3405, 2004.
54. **Sluyter R, Shemon AN, Wiley JS.** P2X$_7$ receptor activation causes phosphatidylserine exposure in human erythrocytes. *Biochem Biophys Res Commun* 355: 169–173, 2007.
55. **Smart ML, Panchal RG, Bowser DN, Williams DA, Petrou S.** Pore formation is not associated with macroscopic redistribution of P2X7 receptors. *Am J Physiol Cell Physiol* 283: C77–C84, 2002.
56. **Sohn DH, Kim HD.** Effects of adenosine receptor agonists on volume-activated ion transport in pig red cells. *J Cell Physiol* 146: 318–324, 1991.
57. **Surprenant A, Rassendren F, Kawashima E, North RA, Buell G.** The cytolytic P$_{2Z}$ receptor for extracellular ATP identified as a P$_{2X}$ receptor (P2X$_7$). *Science* 272: 735–738, 1996.
58. **Tanneur V, Duranton C, Brand VB, Sandu CD, Akkaya C, Gachet C, Sluyter R, Barden JA, Wiley JS, Lang F, Huber SM.** Purinoceptors are involved in the induction of an osmolyte permeability in malaria-infected and oxidized human erythrocytes. *FASEB J* 20: 133–135, 2006.
59. **Wang L, Olivecrona G, Gotberg M, Olsson ML, Winzell MS, Erlinge D.** ADP acting on P2Y$_{13}$ receptors is a negative feedback pathway for ATP release from human red blood cells. *Circ Res* 96: 189–196, 2005.
60. **Wiley JS, Chen JR, Snook MB, Jamieson GP.** The P$_{2Z}$-purinoceptor of human lymphocytes: actions of nucleotide agonists and irreversible inhibition by oxidized ATP. *Br J Pharmacol* 112: 946–950, 1994.
61. **Wiley JS, Dao-Ung LP, Li C, Shemon AN, Gu BJ, Smart ML, Fuller SJ, Barden JA, Petrou S, Sluyter R.** An Ile-568 to Asn polymorphism prevents normal trafficking and function of the human P2X$_7$ receptor. *J Biol Chem* 278: 17108–17113, 2003.